



HAL
open science

Remagnetization of lava flows spanning the last geomagnetic reversal

Jérôme Vella, Julie Carlut, Jean-Pierre Valet, Maxime Le Goff, Vicente Soler,
Fernando Lopes

► **To cite this version:**

Jérôme Vella, Julie Carlut, Jean-Pierre Valet, Maxime Le Goff, Vicente Soler, et al.. Remagnetization of lava flows spanning the last geomagnetic reversal. *Geophysical Journal International*, 2017, 210 (2), pp.1281-1293. 10.1093/gji/ggx212 . insu-02178831

HAL Id: insu-02178831

<https://insu.hal.science/insu-02178831>

Submitted on 10 Jul 2019

HAL is a multi-disciplinary open access archive for the deposit and dissemination of scientific research documents, whether they are published or not. The documents may come from teaching and research institutions in France or abroad, or from public or private research centers.

L'archive ouverte pluridisciplinaire **HAL**, est destinée au dépôt et à la diffusion de documents scientifiques de niveau recherche, publiés ou non, émanant des établissements d'enseignement et de recherche français ou étrangers, des laboratoires publics ou privés.

Remagnetization of lava flows spanning the last geomagnetic reversal

Jérôme Vella,¹ Julie Carlut,¹ Jean-Pierre Valet,¹ Maxime Le Goff,¹ Vicente Soler² and Fernando Lopes¹

¹*Institut de Physique du Globe de Paris (IPGP), Université Paris Diderot, Sorbonne Paris-Cité, UMR 7154 CNRS, 1 rue Jussieu, F-75238 Paris Cedex 05, France. E-mail: carlut@ipgp.fr*

²*Productos Naturales y Agro biología de Canarias, Estación Volcanológica de Canarias, E-38201 La Laguna, Tenerife, Spain*

Accepted 2017 May 17. Received 2017 May 12; in original form 2016 October 27

SUMMARY

Large directional changes of remanent magnetization within lava flows that cooled during geomagnetic reversals have been reported in several studies. A geomagnetic scenario implies extremely rapid geomagnetic changes of several degrees per day, thus difficult to reconcile with the rate of the earth's core liquid motions. So far, no complete rock magnetic model provides a clear explanation. We revisited lava flows sandwiched between an underlying reverse and an overlying normal polarity flow marking the last reversal in three distinct volcanic sequences of the La Palma Island (Canary archipelago, Spain) that are characterized by a gradual evolution of the direction of their remanent magnetization from bottom to top. Cleaning efficiency of thermal demagnetization was not improved by very rapid heating and cooling rates as well as by continuous demagnetization using a Triaxe magnetometer. We did not observe partial self-reversals and minor changes in magnetic grain sizes are not related to the within-flow directional changes. Microscopic observations indicate poor exsolution, which suggests post-cooling thermochemical remagnetization processes. This scenario is strongly reinforced by laboratory experiments that show large resistance to thermal demagnetization when thermoremanence was acquired over a long time period. We speculate that in the present situation exsolution was reactivated during in field reheating and yielded formation of new magnetite, yet magnetic domain state rearrangements could also play a role. Initial reheating when the overlying flow took place, albeit moderate (less than 200–300 °C), was enough to produce overlying components with significantly higher unblocking temperatures.

Key words: Rapid time variations; Remagnetization; Reversals: process, time scale, magnetostratigraphy; Rock and mineral magnetism.

1 INTRODUCTION

Thermoremanent magnetization (TRM) acquisition by lava flows is well understood and described by theory (Néel 1955). It is expected that the direction of remanence is the same throughout the entire flow, provided that cooling did not require more than a few years. Lava flows a few metres thick cool down over a few months period and therefore palaeomagnetic records from superimposed lava units should provide a succession of instantaneous field readings and be used with great confidence. However, subsequent chemical transformations can affect magnetic minerals and/or magnetic stability of grains and generate spurious components of magnetization. Partial remagnetization would remain mostly undetected provided that the geomagnetic variations were moderate or partly time-averaged if they occurred over a long enough time periods. The situation is drastically different in presence of rapid field changes like during geomagnetic reversals or excursions, and it is not surprising that several studies reported anomalous direc-

tional behaviour within flows that took place during periods of geomagnetic reversals.

The first observation by Hoffman (1984) reported variable remanence directions within a transitional flow from the Oligocene Liverpool volcanics in eastern Australia. In this case, post emplacement oxidation could be evidenced by thermal demagnetization. Shortly after, Mankinen *et al.* (1985) and Prévot *et al.* (1985) published a detailed reversal record from the Steens Mountain volcanic sequence initially discovered by Watkins (1965) and that was more recently extended to new sections (Jarboe *et al.* 2011). A puzzling finding was the presence of two large directional gaps while the interior of each flow preceding the gap is characterized by an evolution of the palaeomagnetic directions. The fidelity of the record was advocated in a series of papers (Coe & Prévot 1989; Coe *et al.* 1995; Camps *et al.* 1995) that relied on the absence of changes in magnetic mineralogy within each flow and therefore implied that the field direction changes were as rapid as 1° d^{-1} , i.e. at least two orders of magnitude faster than any

prediction for geomagnetic spikes (Fournier *et al.* 2015). Recently, Coe *et al.* (2014) performed rapid continuous thermal demagnetization using a Triaxe vibrating magnetometer (Le Goff & Gallet 2004) and showed that the within-flow changing directions were caused by incomplete removal of overlapping components. All primary directions were then found to point toward the direction of the underlying lava flow.

Similarities with the Steens Mountain record can be mentioned for several sequences that recorded the last reversal at La Palma (Canary Islands, Spain; Quidelleur & Valet 1996) as well as for the normal-to-reverse polarity transition marking the end of the Cobb Mountain event (1.1 Ma) from Ethiopia (Valet *et al.* 1998). In all sequences, the direction of remanence changes within a flow that is sandwiched between the last flow that recorded the former polarity and the first flow with new polarity. Assuming that these changes occurred during lava cooling, the reversal would have lasted a few months at most, implying field changes of the order of 1°d^{-1} . The lavas share some characteristics with the Steens Mountain and Liverpool flows, particularly the presence of titanomagnetites. However, no very conclusive scenario has been found so far to account for partial remagnetization mechanisms. The issue needs to be addressed further given its frequency. Lava flows are frequently sampled more or less at the same level, and therefore dispersion generated by early post-cooling remagnetization can easily be underestimated.

In this paper, we investigate further two flows from La Palma Island that were previously discussed (Valet *et al.* 1998). In light of the recent studies mentioned above, we perform additional experiments and mineralogical investigations aimed at testing the consequence of slow thermal demagnetization and the existence of self-reversal mechanisms. We add detailed microscopic examinations along with remagnetization experiments that emphasize the role played by small reheating of the overlying flow in presence of partial exsolution.

2 PREVIOUS WORK AND SAMPLING

La Palma Island is located at the east of the Canary archipelago (Fig. 1). The volcanic flows of the Upper Old Series in the Northern part of the island are dated between 1 and 0.7 Ma (Abdel-Monem *et al.* 1972). Several lava flow sequences recorded the last geomagnetic reversal. A previous magnetic study of flows LS108–LS117 (Quidelleur & Valet 1996) from a sequence of 21 units at Los Sauces identified the last reversal between LS111 and LS113. The 2 m thick LS112 unit is sandwiched between a reverse and a normal polarity flow and characterized by within-flow changing directions.

Similar characteristics were reported from the study of another succession of 20 superimposed flows that outcrop near the village of Tricias (Quidelleur & Valet 1996). Anomalous changing directions were again observed within the flow TR10 (Valet *et al.* 1998) that lie between the reverse polarity flow TR9 and the normal polarity flow TR11. Detailed rock magnetic studies were previously conducted on the two critical flows LS112 and TR10 (Valet *et al.* 1998). Despite interesting information and converging observations between the two sections, no complete scenario explains so far the origin of the strongly resistant overlapping components.

Recent suggestions regarding the possible existence of extremely rapid field changes during reversals (Sagnotti *et al.* 2014) in parallel with a new rock magnetic scenario for the Steens Mountain

peculiar flows (Coe *et al.* 2014) led us to revisit these two sequences. We took 35 samples as close as possible to each other along two vertical parallel transects between the top and bottom of flows LS112 and TR10 that were renamed LST and TRC, respectively. The position of each sample was carefully measured from below the top of the flows so that all specimens could be correlated with each other as well as with measurements from the former studies.

The specificity of the present work was to use very tiny specimens in order to conduct multiple experiments on several twin samples and to minimize heating duration. We cut each 25 mm diameter and 25 mm long core into two 11 mm thick discs. Each disc was subsequently drilled using a 6 mm diameter bit. This technique provided six tiny samples from each original core.

3 MAGNETIZATION COMPONENTS

As magnetization of lava was acquired during cooling in the ambient field, we mostly performed thermal demagnetization. All measurements were performed in the IGP shielded room using a 2G cryogenic magnetometer. Samples from Quidelleur & Valet (1996) were added to broaden the set. In Figs 2 and 3, demagnetization characteristics of samples within the flows LST and TRC are shown. On the left-hand side of each figure we show thermal demagnetization diagrams (Zijderveld 1967; Cogné 2003) of samples located at increasing depths in the interior of the flow as indicated in the composite column. On the right-hand side is plotted the evolution of the reversal angle (away from the direction of the present axial dipole at the site) that was derived from the interpretation of the ‘pseudo-characteristic’ component. The corresponding stereo plots compare the high-temperature directions with the low to middle temperature overprint.

The first remark is that the characteristic component is opposite between the base and the top of both flows. Assuming that the true direction was recorded and preserved at the base of the flows, we expect a reversed polarity within the entire flow. Under this assumption, the overlying samples are either partially or fully remagnetized and total remagnetization with full normal polarity is clearly observed at the levels close to the overlying flow. The samples located between 26 and 50 cm below the top of LST flow show a resistant overprint with positive inclinations and declinations between 60°E and 90°E . As we get closer to the bottom of the flow a high-temperature component with reversed inclination emerges progressively like in sample LST07 at 53 cm below the top, but not with full reverse polarity. Interestingly, the lower region of TRC flow is characterized by normal remagnetization of higher magnitude as reverse directions are barely recorded. Note that this flow is thinner than LST.

In both cases, alternating field (a.f.) demagnetization did not improve the determination of the characteristic component. A typical example is shown in Fig. S1 in the Supporting Information that compares the demagnetization diagrams of two specimens located 36 cm below the top of flow LST. Demagnetization by a.f. seems to be more efficient to remove the softer component that is likely carried by coarser grains, but it fails to isolate the reverse polarity that was recorded at the bottom of the flow.

As previously mentioned (Valet *et al.* 1998), the results point out the presence of partial or complete remagnetization within a large part of the flow. Reheating by the overlying flow comes first to mind and can be defended since the importance of remagnetization

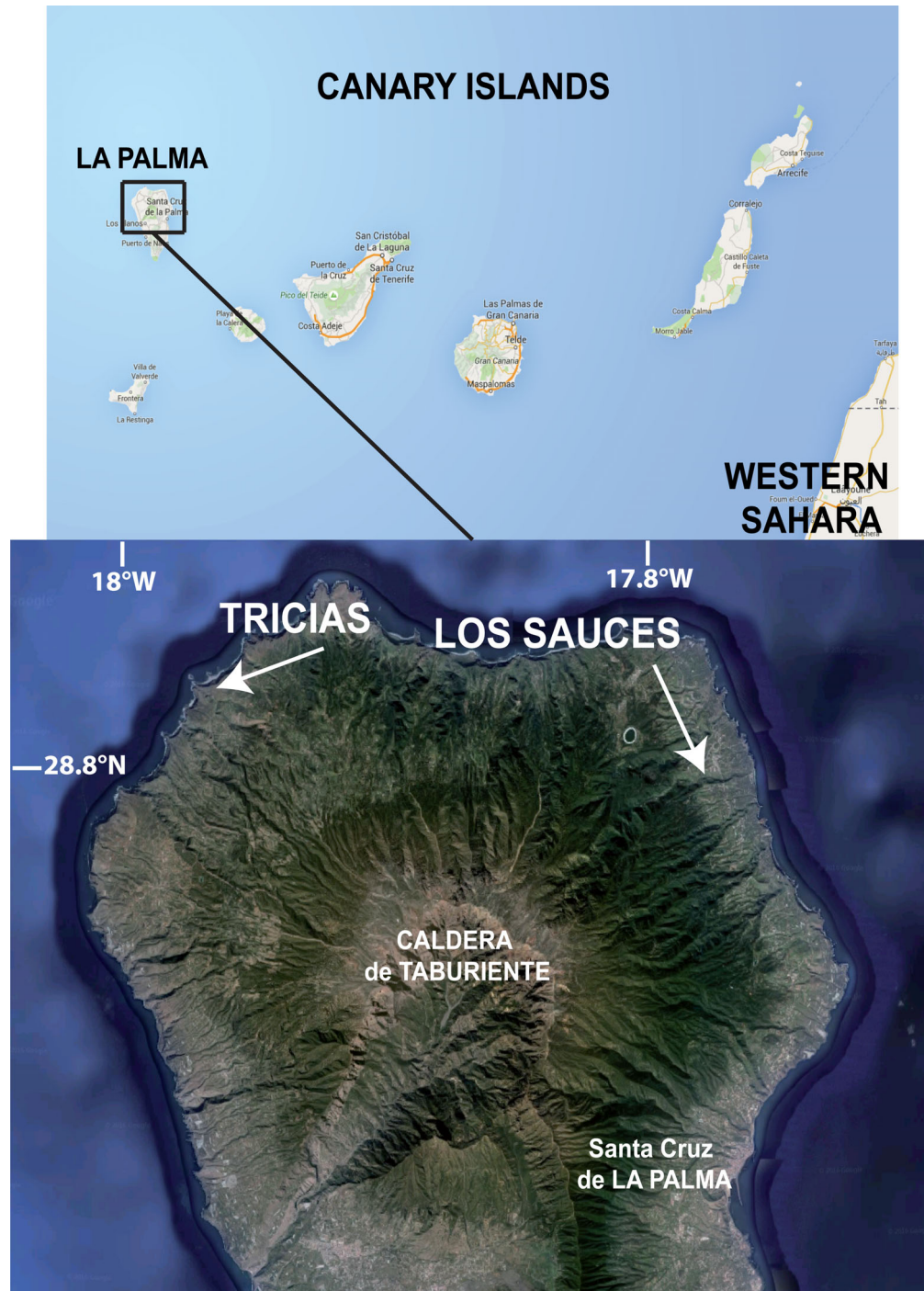


Figure 1. Sampling sites locations (plotted using Google Earth data).

decreases with depth. However, the vertical extent of remagnetization and the persistence of very high unblocking temperatures are difficult to account by this unique scenario (Valet *et al.* 1998). Other processes must have occurred after emplacement.

4 INFLUENCE OF HEATING RATE DURING THERMAL DEMAGNETIZATION

Following recent results on the efficiency of thermal demagnetization with fast heating (Coe *et al.* 2014), we tested whether similar

effects would explain the behaviour of the La Palma flows. We used two distinct approaches and performed (i) traditional step-wise demagnetization in zero field using tiny specimens and different heating times and (ii) continuous thermal demagnetization and measurements.

Three series of specimens obtained from the same samples were successively heated in zero field for 15, 30 and 60 min and measured. The samples were always positioned at the same location within the oven. The first heating step was set at 350 °C to avoid minor changes that could be generated by successive heatings at lower temperatures. Fifteen minutes heating time were used at 350, 450,

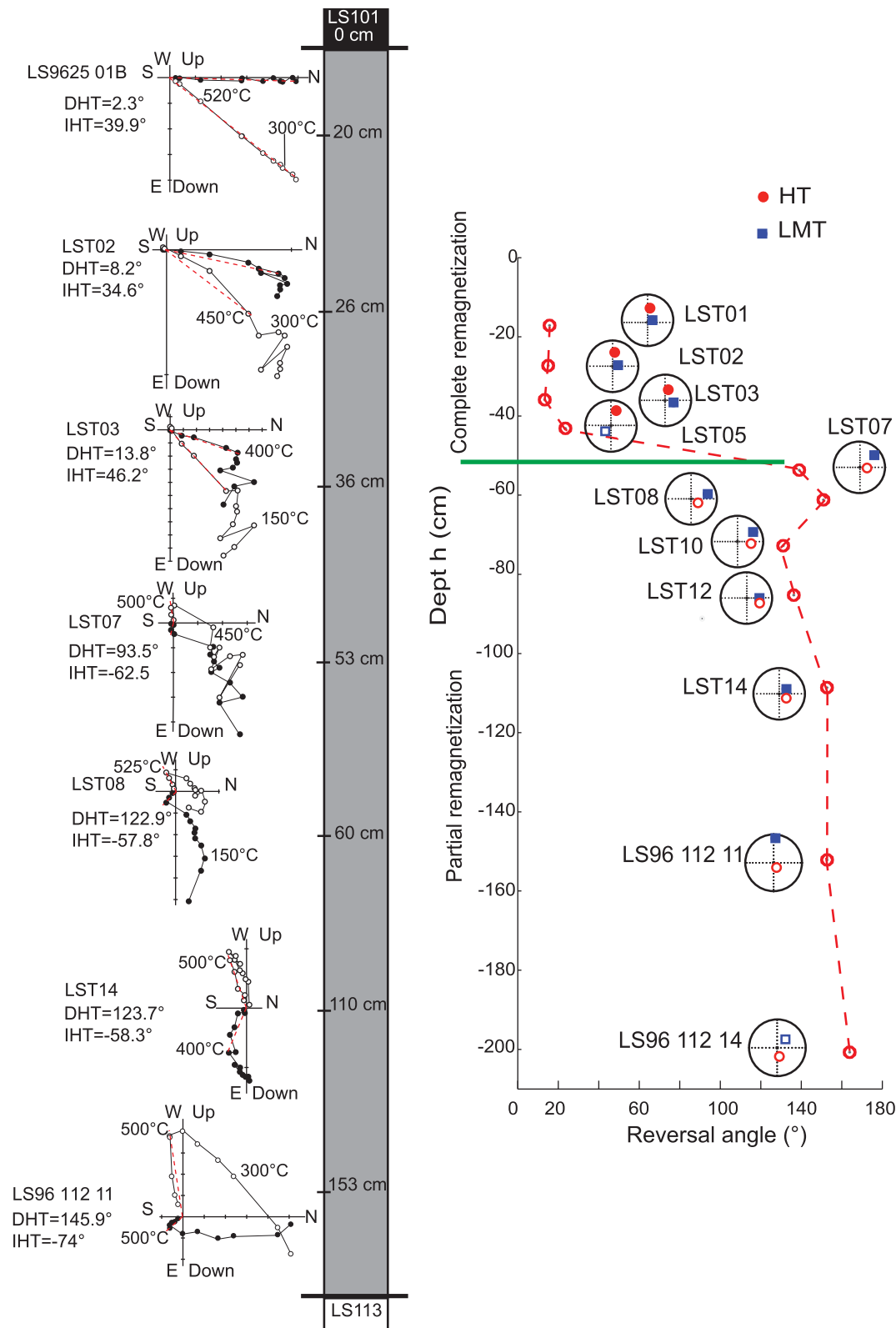


Figure 2. Evolution of the directions within flow LST. On the left-hand side are plotted the demagnetization diagrams obtained after stepwise thermal treatment at the depth indicated in the grey column. Samples named after LST LS96 represent specimens measured in Valet *et al.* (1998). The stereographic plots on the right-hand side show the directions of the low- (blue) and high-temperature (red) components, while the dotted red line indicates the evolution of the reversal angle of the characteristic directions derived from the HT components (that represent the angular deviation away from the direction of the axial dipole at the site). The results indicate normal polarity down to 50 cm from the top of the flow and reversed polarity at the bottom.

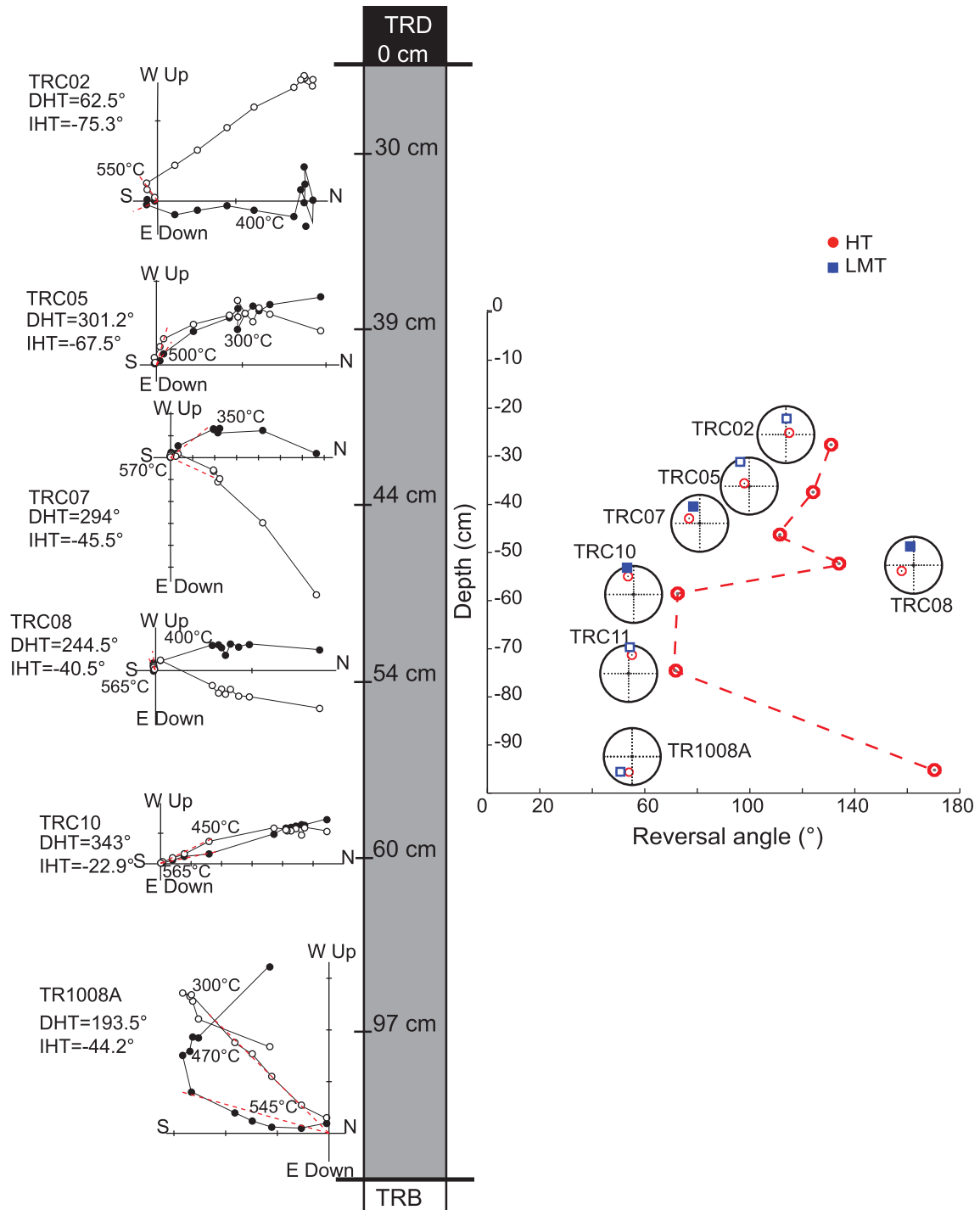


Figure 3. Same as Fig. 2 for flow TRC.

480, 510, 550, 565 and 580 °C, while 30 min heating times were directly performed at 540 °C with successive 5 °C incremental steps up to 580 °C in order to target the high-temperature component. Classical thermal demagnetization performed for 1 hr by 'standard' steps of 50 °C from 100 to 500 °C, then every 25–15 °C was also performed for comparison.

We then turned towards the Triaxe technique in order to speed up the process further. We basically followed the same approach and used the same device as for the experiments performed by Coe *et al.* (2014), thereby providing the possibility of comparing

the two sets of measurements. The Triaxe vibrating magnetometer (Le Goff & Gallet 2004) allows rapid and automatic demagnetization and measurements of tiny cylindrical samples (~0.75 cm long and 1 cm diameter) with magnetization as low as 10^{-8} A m². Measurements are performed during heating so that complete demagnetization can be reached in ~12 min with a 60 °C min⁻¹ heating rate. At least, one sample from the base, from the middle and from the top of the flows was selected for this technique. Full description of the Triaxe data treatment can be found in Le Goff & Gallet (2004).

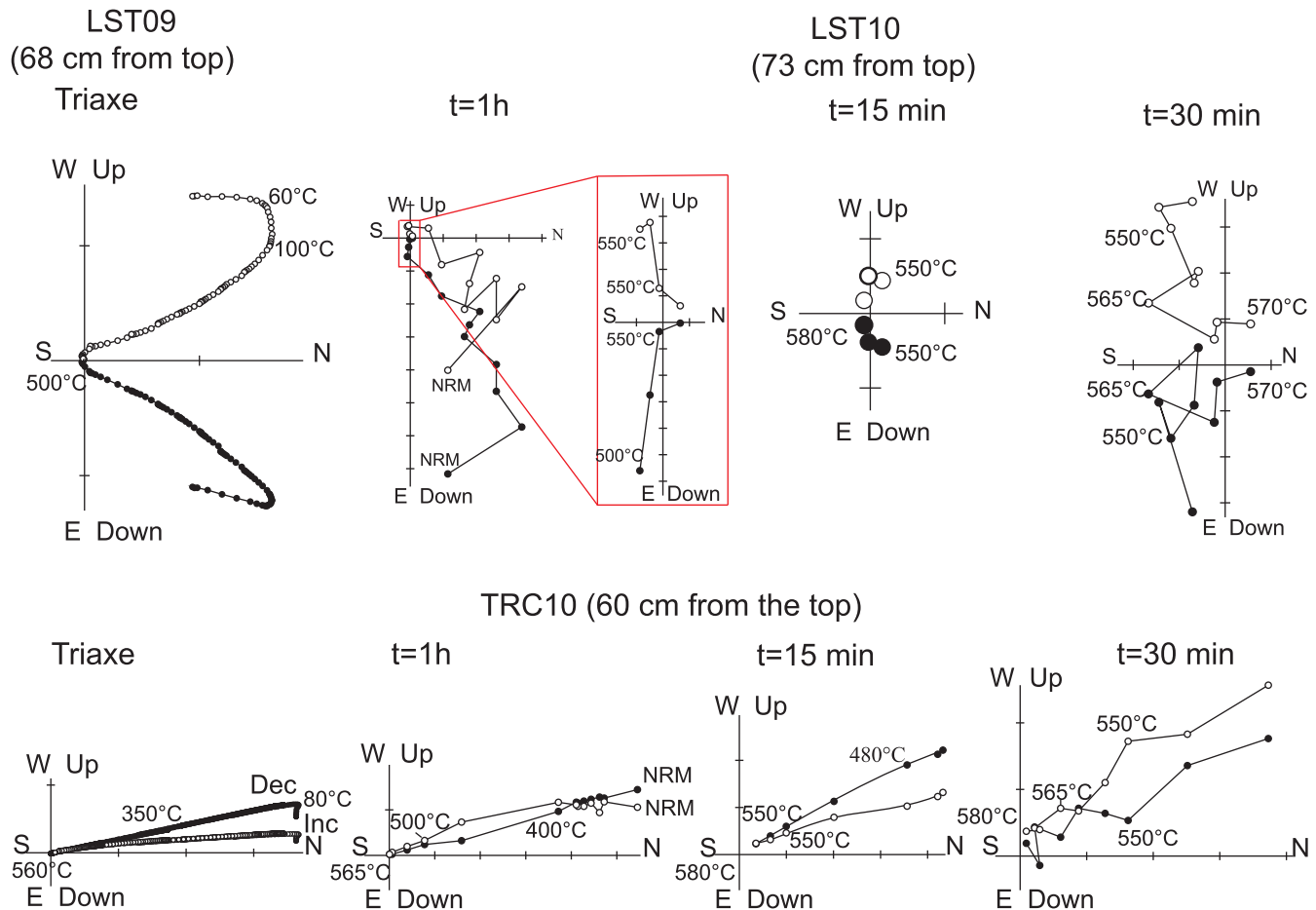


Figure 4. Comparison of demagnetization characteristics for different heating times. From left to right are shown the demagnetization diagrams of twin samples obtained after continuous thermal demagnetization, 1 hr, 15 min and 30 min heating times, respectively. Short heating times as well as continuous thermal demagnetization did not improve the demagnetization and failed to isolate the reverse polarity primary component.

The results of the four successive experiments are compared in Fig. 4 for two batches of samples that are at about the same distance from the top of both flows. We note first that the Triaxe did not improve the efficiency of thermal demagnetization. A tiny high-temperature component emerges beyond 550 °C in samples LST09 and LST10, but it is poorly constrained for all protocols with a direction intermediate between the two polarities (note that the declination differs between the two LST samples because they were not taken exactly at the same depths). The same remark holds for the TRC10 sample that, despite being 60 cm below the top, keeps a normal polarity direction during the entire demagnetization. We infer that changing the heating rate and the measurement technique did not change the magnetization characteristics during and after demagnetization. In contrast with the Steens Mountain experiments, no viscous component induced during heating could be detected and therefore different processes might be involved.

5 ROCK MAGNETIC CHARACTERISTICS

5.1 Magnetic mineralogy

Thermomagnetic measurements were conducted in air up to 650 °C using a KLY-3/CS-3. In Figs 5(a) and (b), we can compare the evolution of natural remanent magnetization (NRM) during thermal

demagnetization with the thermomagnetic susceptibility behaviour of samples within the two lava flows. The results are similar in both cases. The specimens located close to the edges of the flows are characterized by strong resistance to thermal demagnetization and a rapid decrease of their remanent magnetization down to 580 °C with a narrow range of high unblocking temperatures. These results suggest that the magnetization is fully dominated by magnetite. The inner parts of the flows show a different pattern with a smoother decrease of the remanent magnetization. The evolutions of susceptibility and remanence with temperature show two or three slopes, the first one being likely related to titanomagnetite, while the second one may simply result from overlapping medium- and high-temperature components. In all samples from the inner part, the last slope beyond 480 °C involves a little amount of magnetization compared to the top and bottom samples. We infer that these samples contain a lower amount of pure magnetite and that the presence of titanomagnetite cannot be neglected. Most samples have lower susceptibility values during cooling than during heating that may result from oxidation processes during heating. The difference is enhanced for samples that are richer in titanomagnetite. Except the very top of the flow, the samples from TRC are also characterized by a sharp decrease of magnetization below 100 °C that is even visible at the interior of the flow. It is associated with a little bump in the thermomagnetic curves that could reflect the presence of titanomagnetite with high titanium content or possibly goethite (De Boer & Dekkers 1998).

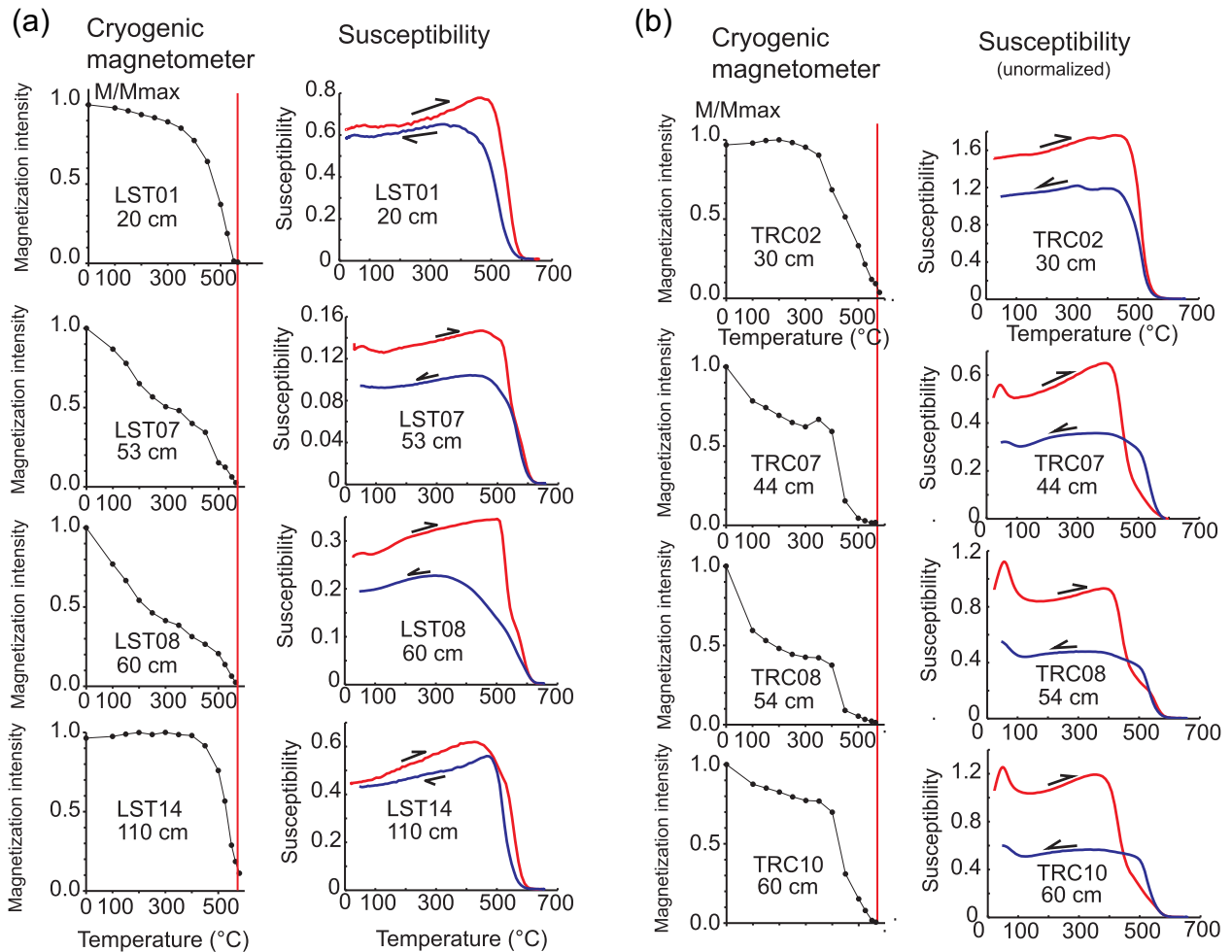


Figure 5. (a) Evolution of the intensity of remanence during stepwise thermal demagnetization and of low field susceptibility during thermomagnetic experiments for samples from the interior of flow LST. Both parameters are similar in the samples from the top and bottom of the flow and indicate the dominance of almost pure magnetite. In contrast, the magnetic moments of the two samples from the middle of the flow show an inflexion indicative of titanomagnetite and larger production of magnetite after heating. (b) Same as (a) for flow TRC.

5.2 Scanning electron microscope observations

Four polished thin sections from LST (LST01 and LST07) and TRC (TRC05 and TRC11) series were studied using a Zeiss Auriga scanning microscope in backscattered mode equipped with calibrated (Cu standard) energy-dispersive X-ray spectroscopy (EDS-X) Bruker detectors. In all four samples, most iron oxides are a few micrometres in size (typical range is 1–20 μm , Fig. 6a). EDS-X analyses show that titanium is almost always associated with iron oxides with varying concentration. Most analyses indicate stoichiometry in the range $\text{Fe}_{2.5}\text{Ti}_{0.5}\text{O}_4$ (TM50) to $\text{Fe}_{2.1}\text{Ti}_{0.9}\text{O}_4$ (TM90). Such high titanium content corresponds to magnetic phases with low Curie temperatures, from below room temperature to $\sim 300^\circ\text{C}$ (O'Reilly 1984), exsolution and oxidation can however significantly increase these temperatures. High magnification revealed that a large proportion of grains from LST01 have small exsolutions (Fig. 6b) with domains a few hundred of nanometres size associated with low Ti concentration that likely carry most of remanent magnetization. Only few exsolutions were observed within the iron oxides from LST07, TRC05 and TRC11 despite intensive observations (Figs 6c–e). Even at the highest magnification scale (Fig. 6c), most grains are homogeneous high-Ti magnetite. In many cases, thin filaments (possibly elongated prism corresponding to filing of cracks) with

lighter colour were observed (Figs 6c–f) with sizes ranging from 100 to 200 nm (Fig. 6f). The EDS-X analyses indicate that this phase is an iron oxide with low titanium content. It likely represents low Ti-magnetite/maghemite or alternatively haematite as suggested by Krása *et al.* (2005) who reported similar observations. This phase is presumably the result of iron diffusion during an episode of moderate titanomagnetite alteration.

5.2 Hysteresis and isothermal remanent magnetization

Hysteresis loops and acquisition of isothermal remanent magnetization (IRM) were measured on small chips (~ 250 mg) using a VSM/AGM instrument. The hysteresis loops and the IRM measurements indicate almost total saturation of the remanence by a 200 mT field for the LST samples (with the exception of LST14 which tend to be saturated by a slightly higher field of ~ 300 mT) and 150 mT for the TRC samples (Fig. S1, Supporting Information). Analysis of the IRM acquisition curves using Cumulative Log Gaussian functions (Kruiver *et al.* 2001) confirms the low coercivity of the magnetic carriers with $B_{1/2}$ (that represent the field corresponding to half SIRM) values ranging from 50 to 75 mT for the LST samples and from 20 to 30 mT for the TRC samples without meaningful within flow variations. Hysteresis parameter ratios

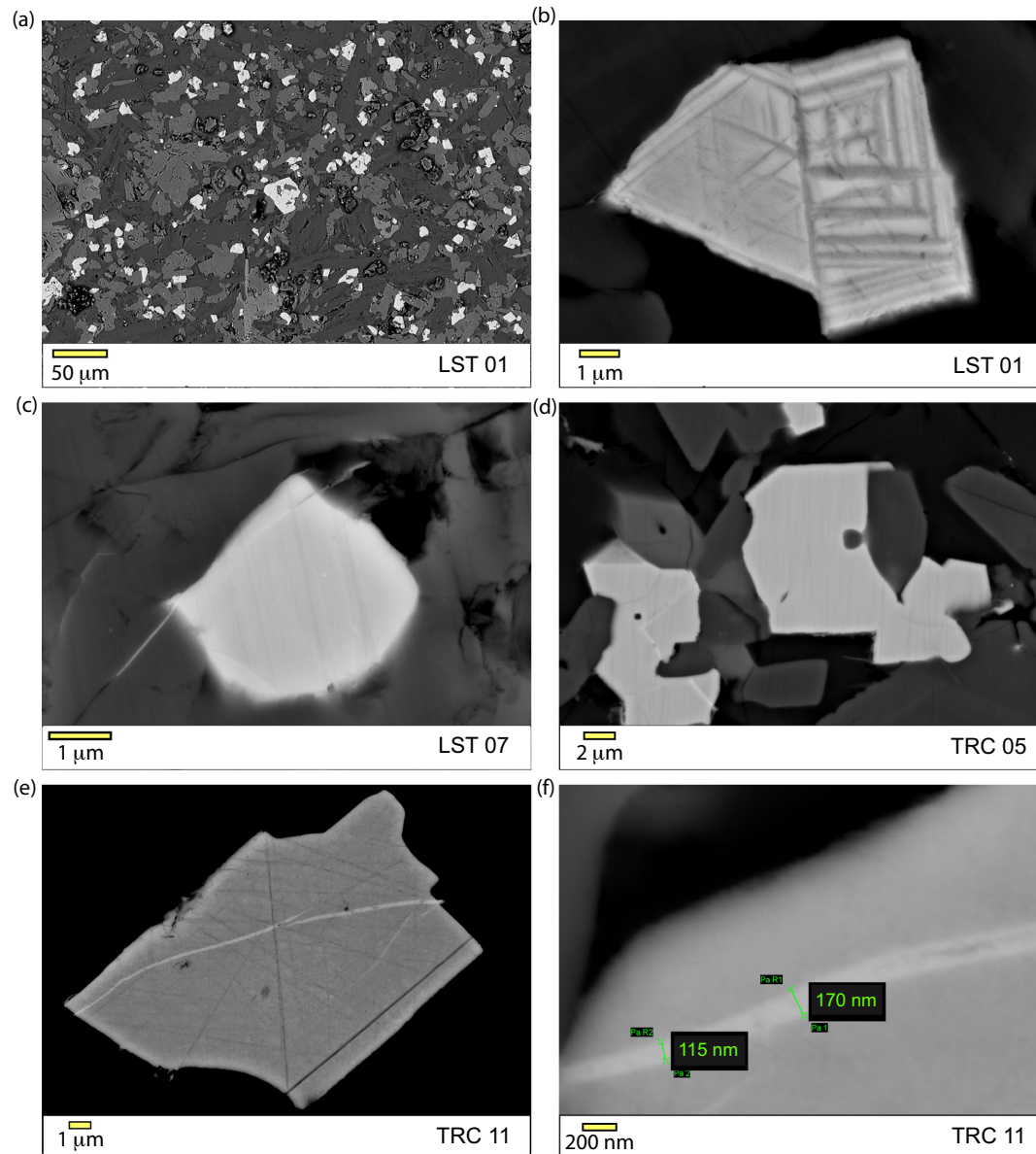


Figure 6. Scanning electron microscope (SEM) images in backscatter mode. (a) Low magnification view of LST01, iron oxides appear white; (b) ilmenite-lamellae in titanomagnetite host from LST01; (c) unexsolved titanomagnetite in LST07, a crack is observed in the upper right of the grain; (d) same as (c) in TRC05; (e) and (f) details of sample TRC11 showing titanomagnetite grains with narrow cracks filled by a secondary bright mineral, clearly distinguishable from polishing marks (black lines). Measurements show that cracks are 100–200 nm wide.

(J_{rs}/J_s and H_{cr}/H_c) lie within a small area ($0.18 < J_{rs}/J_s < 0.32$ and $1.7 < H_{cr}/H_c < 2$) of the single-domain/multi-domain (SD/MD) mixing zone (corresponding to ~30 per cent up to 50 per cent of MD) defined by Dunlop (2002), except for the uppermost samples from both flows which show opposite tendencies that are difficult to interpret since assemblages of magnetic grains with different compositions can bias the analysis of hysteresis parameters in terms of magnetic grain sizes (Fig. S2, Supporting Information). Excluding the uppermost samples, the hysteresis parameters do not depict any clear tendency with their position within flow.

5.3 Viscosity test

In order to evaluate the contribution of magnetic carriers with short relaxation times, we relied on the viscosity test de-

signed by Thellier & Thellier (1944). Samples were stored in the IPGP shielded room in a ~300 nT field and remanence (NRM1) was measured after two weeks. Then, the samples were stored in the laboratory field (55 μ T) for another two weeks and measured again yielding NRM2. The viscosity index $V = (|NRM2 - NRM1|)/|NRM1|$ derived from all experiments show the same evolution within both flows (Fig. S3, Supporting Information). Viscosity increases from the top to the middle of the flows, with a maximum of 2.1 per cent for LST and 1.3 per cent for TRC. It is lower than 1 per cent at the bottom. These weak values indicate that a minor proportion of grains with low relaxation times could have been remagnetized. However, the contribution of this tiny fraction was likely removed below 300 °C, and therefore cannot be responsible for large amplitude directional changes.

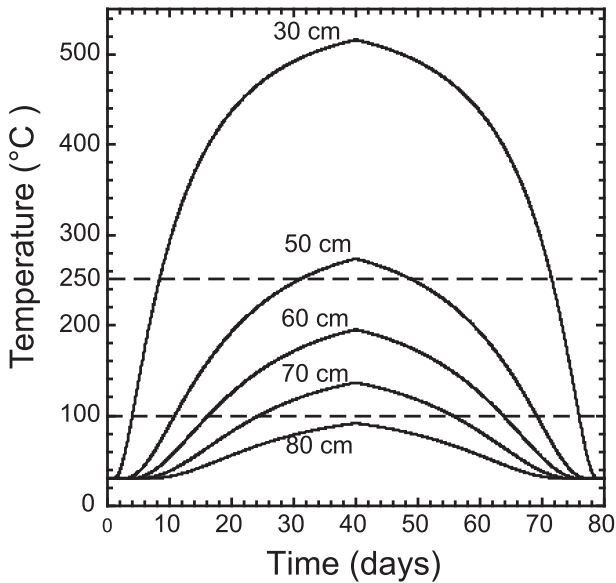


Figure 7. Time evolution of temperature profiles within a lava flow baked by a 2 m thick lava emplaced at 1200 °C at day = 0. Dashed lines mark the 100 and 250 °C limit.

6 REMAGNETIZATION BY REHEATING

6.1 Thermoviscosity

Consequences of reheating by the overlying flow were previously discussed in Valet *et al.* (1998) on the basis of a simple conductive model (Shaw *et al.* 1977). In order to simulate at best the situation of the present sequences, we reinvestigated the evolution of temperature within a flow capped by a 2 m thick flow that takes place at 1200 °C using a more comprehensive model based on markers cell technique described in Gerya (2009) that includes conductive and radiative processes. The results (Fig. 7) show that reheating at 500 °C was restrained within the upper 30 cm. Below 80 cm, the reheating temperature do not exceed 100 °C and should thus remain barely notable during palaeomagnetic investigations. However, medium temperatures of ~250 °C could be reached down to 50 cm and maintained for two weeks. Duration of TRM acquisition at a given temperature is a critical parameter that constrains the unblocking temperature spectrum. Theoretical predictions of relaxation times for identical SD magnetite (Pullaiah *et al.* 1975) indicate that unblocking temperatures of a TRM acquired during a few weeks should not exceed the blocking temperatures by more than 50 °C. However, a more realistic relaxation time/blocking temperature model for SD magnetite (Middleton & Schmidt 1982) with a lognormal distribution of grain size that is compatible with our scanning electron microscope (SEM) observations indicates that reheating at 250 °C during a 2 weeks period can raise the maximum unblocking temperatures up to 400–450 °C. Experiments also show that a population of 20 µm average grain size pseudo-single domain (PSD) magnetite has a maximum unblocking temperature that is 150 °C above their blocking temperature after only 3.5 hr heating time (Dunlop & Özdemir 2000). Summarizing, thermoviscous effects could thus be partly responsible for a remaining high-temperature overprint, possibly up to 400–450 °C but they do not explain total remagnetization with unblocking temperatures that reach 580 °C.

6.2 Chemical remagnetization

Another hypothesis is that moderate reheating by the overlying flow generated magnetochemical transformations within the underlying flow. We did not observe clear secondary minerals that would support the hypothesis of chemical remagnetization in the La Palma flows. However, unexsolved titanomagnetite dominates in the middle of the flows while the lower and upper parts are dominated by magnetite, which indicates that oxy-exsolution was more effective there. Curie temperature and microscope observations by Böhnell *et al.* (1997) on samples from a 6.5 m uncapped flow of the Xitle volcano (Mexico) have shown that the titanomagnetite and ilmenite crystals had a higher oxidation state in the middle of the flow than crystals at the topmost levels. Similar observations were made by de Groot *et al.* (2014) on a 6 m thick inflated uncapped lava flow at Hawaii. Biggin *et al.* (2007) emphasized that such differences in the oxidation state of magnetic carriers reflect differences in cooling rate. Heat transfer in the interior and basal part of subaerial lavas is driven by conduction, while the upper tens of centimetres of the flow cool very rapidly by convection, radiation and conduction into the atmosphere, thus without possible oxidation and leaving most titanomagnetite crystals unexsolved. This is not the case for the LST and TRC flows where samples from the top region were more exsolved than in the middle region. We speculate that the lower region of these thin flows partly exsolved due to long conductive cooling, but that their middle and upper parts remained largely unexsolved due to rapid cooling. Then, a fraction of titanomagnetite was subsequently exsolved in the upper part during reheating by the above flow. Exsolution remained partial in the interior of the flow but sufficient to generate chemical remanent magnetization (CRM) acquisition with high blocking temperatures. If this scenario is correct, we can speculate that subsequent reheating in laboratory should reactivate the process, especially for the middle region of the flow, and significantly raise blocking temperatures.

7 LABORATORY REMAGNETIZATION EXPERIMENTS

Two samples from the middle region and one sample from the upper region from each flow were selected for this experiment. We first removed as much TRM as possible from all samples in order to get a residual signal. After demagnetizing the initial NRM by 150 mT a.f. peak fields, the remaining magnetization (NRM_{150 mT}) was on the order of 10⁻² A m⁻¹ in all samples and the NRM/NRM_{150 mT} ratios were comprised between 15 and 50.

The same samples were subsequently heated at 250 °C in a 56 µT field aligned along the axis of the cylindrical oven for 8 d. Then, the field was turned off and, a few seconds later, the oven was set to decrease to room temperature in zero field, similarly to classical thermal demagnetization (Fig. 8a). This kind of experiment is typically set to detect heating remanence (HRM). If a fraction of magnetic grains were activated during field heating and their magnetization blocked at temperatures above 250 °C, the new magnetization (HRM_(250 °C; H = 56 µT)) should have increased. After measuring the HRM_(250 °C; H = 56 µT), the samples were stepwise thermally demagnetized by heating in zero field for 90 min at 20 °C incremental steps between 250 and 510 °C.

In Fig. 8, we plot the remaining magnetization, normalized to HRM_(250 °C; H = 56 µT), after each 90 min thermal demagnetization step. All samples show stronger magnetization after the experiments and higher T_{ub} (unblocking temperature) than T_b (blocking temperature). The increase in magnetization for the HRM_(250 °C; H = 56 µT)

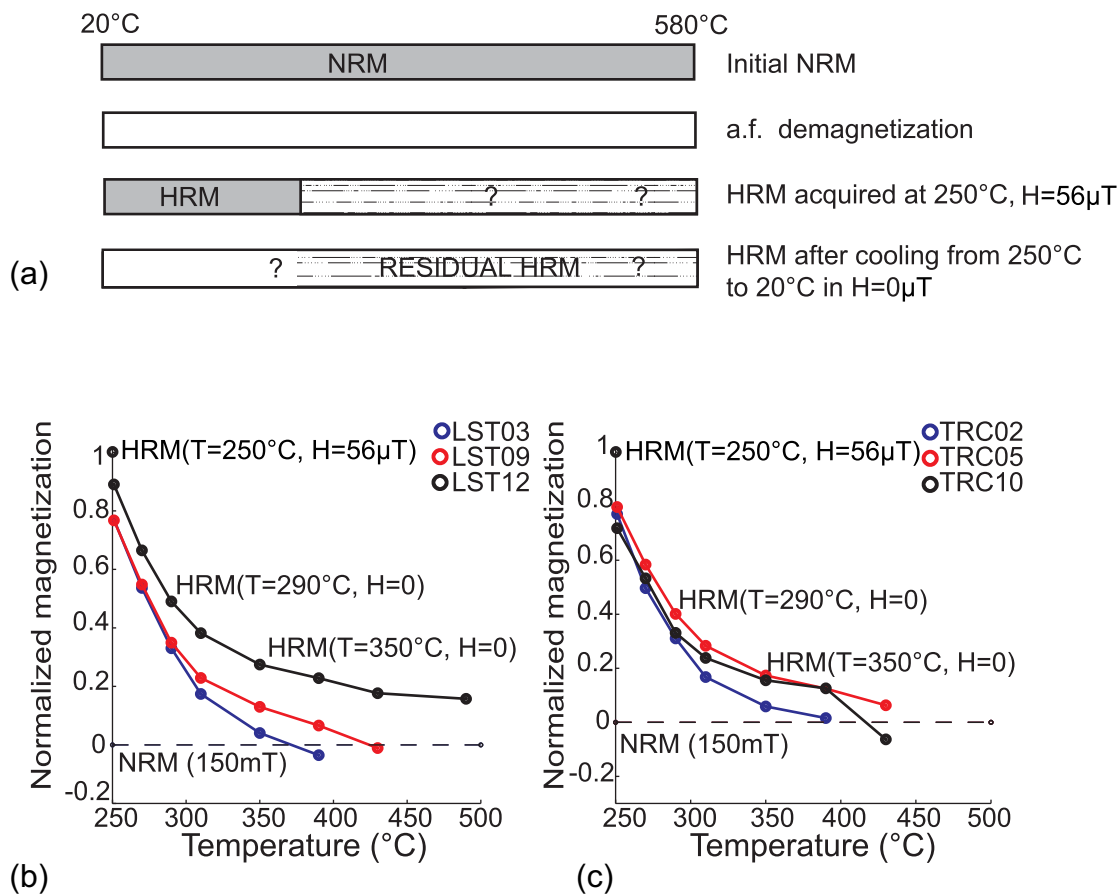


Figure 8. (a) Schematic representation of the successive heating and cooling with and without field during a remagnetization experiments. (b) and (c) Demagnetization curves of HRMs produced at increasing temperatures for a series of three samples from flows (b) LST and (c) TRC. The per cent ratios of the HRM (produced by a 56 mT field at 250 °C over 8 d period followed by cooling in zero field) over the initial NRM are (LST03: R = HRM/NRM = 10 per cent; LST09 R = 28 per cent; LST12 R = 50 per cent; TRC02 R = 15 per cent; TRC05 R = 60 per cent and TRC10 R = 11 per cent).

is about 10 times the $NRM_{150\text{ mT}}$ and can reach significant values from about 10 per cent of initial NRM (for LST03 and TRC02) up to 50 and 60 per cent (for LST12 and TRC05, respectively). By contrast, we observed only a very moderate 1–3 per cent increase in bulk susceptibility after heating, which confirms that no major mineralogical changes happened during heating as expected from the thermomagnetic measurement results (Section 5.1). About 20 per cent of the HRM magnetization was lost during the 90 min long first heating run at 250 °C. The samples from the upper region (LST03 and TRC02) were heated up to 350 °C to reach a magnetization level equivalent to that of $NRM_{150\text{ mT}}$. It is even more striking that the resistance of the samples from the interior of the flows (LST09, LST12, TRC05 and TRC10) exceeded the predictions of the thermoviscous models (Pullaiah *et al.* 1975; Middleton & Schmidt 1982). Almost 20 per cent of magnetization of sample LST12 persisted after heating in zero field at 400 °C. Similarly, the data from TRC (Fig. 8c) confirmed the presence of grains with large T_{ub} in the interior of the flow.

8 DISCUSSION

Except the large within-flow dispersion of the palaeomagnetic directions, the pseudo-characteristic components that were isolated from the LST and TRC flows meet standard criteria of reliability: high-temperature characteristic remanent magnetization (ChRM)

carried by magnetite and/or titanomagnetite, and directions pointing towards the origin of the demagnetization diagrams. The reverse directions of samples LST14 and TRC11 at the base of the LST and TRC flows are the most remote from the overlying normal polarity flow. They are both carried by single-domain magnetite with high unblocking temperatures and consequently clearly predate the above normal polarity period. We infer that these directions are truly representative of the reverse polarity field prior to the transition. Conversely, the normal polarity directions found in the upper part of the flows are not believed to be reliable.

The directional changes within the B51 Steens Mountain flow range from reverse to normal to transitional. Continuous thermal demagnetization performed with a Triaxe magnetometer revealed that a residual viscous remanent magnetization (VRM) was mixed with the primary TRM that could not be properly isolated after stepwise thermal demagnetization. The high-temperature component isolated by continuous demagnetization kept the same reverse direction in all samples and was consistent with the reverse polarity of the underlying flow. Coe *et al.* (2014) suggested that the characteristic reverse component was screened after alteration of magnetic grains carrying an overprint during stepwise thermal demagnetization in the laboratory. Due to the high unblocking temperatures of the overprinted grains, the spurious components could not be separated from the primary remanence.

We discussed in Section 4 that both thermal demagnetizations with very short heating times and continuous measurements using

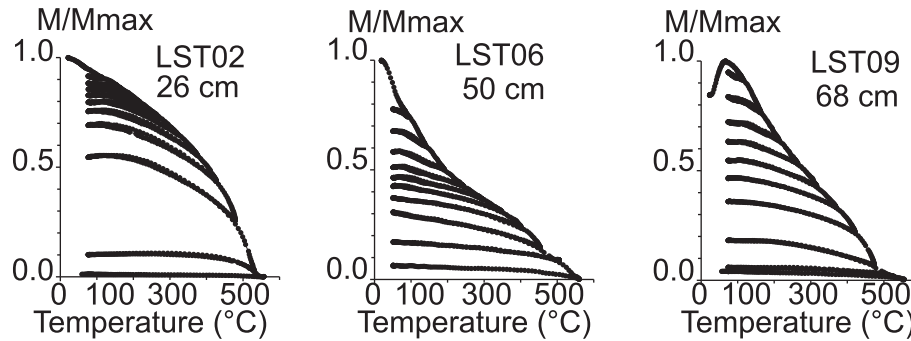


Figure 9. Evolution of the NRM (normalized) for samples LST02, LST06 and LST09 during continuous thermal demagnetization using the Triaxe vibrating sample magnetometer. Heating–cooling cycles are performed to progressively higher temperatures up to 550 °C.

the same protocol as in Coe *et al.* (2014) confirmed the determinations derived from standard stepwise thermal demagnetization. In addition, stepwise demagnetization by a.f. yielded similar results. Therefore, the scenario proposed by Coe *et al.* (2014) for the abnormal behaviour of Steens Mountain flows is not relevant for the LST and TRC flows.

Partial self-reversal can be envisaged as an alternative explanation. A scenario drawn by Krása *et al.* (2005) involves a non-oxidized or slightly oxidized pristine titanomagnetite (mother phase) and an oxidized titanomaghemite (daughter phase). During acquisition of remanence, the two phases are magnetically coupled so that the low Curie temperature phase (mother phase) acquires a magnetization that is antiparallel to the external field. Narrow (50–200 nm) bands filled with low Ti iron oxide within titanomagnetite are an ubiquitous observation in our samples and strikingly resemble the microscopic observations by Krása *et al.* (2005). The crack filling daughter phase separates the magnetic grain in two (or more) domains. Analytical and numerical calculations indicated that this could be responsible for self-reversed remanent magnetization that was observed in Krása *et al.* (2005) samples. However, this model implies that partial or complete self-reversal cannot be detected by standard stepwise demagnetization in zero field, but is clearly visible when performing continuous measurements. Therefore, no significant problem is expected for the NRM under this scenario, since the upper part of the temperature spectrum carries a reliable magnetization. This is actually opposite to the situation of La Palma as well as Steens Mountain flows that do show distinct directions in the flow interiors that are neither parallel nor antipodal to those of the overlying and underlying units. The most significant observation is that the cooling curves of the continuous measurements (Fig. 9) of the La Palma samples do not show any decrease of remanent magnetization that would be indicative of self-reversal. We infer that processes yielding self-reversals if any are extremely limited and did not generate dispersion of directions within flow.

In our study, the remagnetization experiments performed in laboratory suggest that a high-temperature remagnetization component was possibly generated after medium temperature (250 °C) reheating during a few days only. This could be caused by (1) typical MD viscous effects, (2) thermochemical processes due to exsolution and/or growth of new phases, (3) transdomain remanence following changes in magnetic domain configurations of some grains (Moon & Merrill 1986; Calvo *et al.* 2002; de Groot *et al.* 2012).

Viscous effects are mostly due to large multidomain grains, but there is no obvious reason for accumulating large multidomain grains in the middle of thin lava flows. Their presence is neither indicated by the hysteresis parameters, nor by the characteristics derived from a.f. demagnetization, IRM measurements and SEM

observations. Furthermore, large MD thermoviscous magnetization is a ‘soft’ and low magnitude remanence that should not be resistant to moderate a.f. demagnetization steps. It is a possibility that the flows were erupted during a period of weak Earth magnetic field and that in subsequent times a field of higher magnitude enhanced any MD tail effects but the stable and strong magnetization of the samples suggests other causes.

Hoffman (1984) has reported similar within-flow directional changes and proposed that the anomalous directions found in the 35 Ma old Liverpool flow (Australia) resulted from only partial exsolution of titanomagnetite during emplacement and cooling of lava. Subsequent oxidation at room temperature proceeded at varying rates and generated new low-titanium magnetite grains that acquired a CRM with either normal or reversed polarity. Low-temperature exsolution was thus a dominant mechanism for remanence acquisition in a large part of the flow. A common characteristic with the Liverpool lava flow is the presence of high Ti titanomagnetite that was identified in our samples from SEM observations. A dominant feature is that the remanence of the samples from the lower and upper levels of the flow is carried by pure magnetite but with almost opposite polarities (reverse at the bottom and normal at the top), while the samples from the middle of the flows contain titanium and display erratic directions of magnetization. Subtle exsolutions especially within the smallest grains that were caused by heating are interesting candidates for the La Palma flows. The small grain exsolved phases would significantly contribute to a stable and resistant magnetization up to high temperatures, but such transformations may be difficult to detect in laboratory. Susceptibility might not be very discriminant as the signal is dominated by large grains and conversion of small amounts of intermediate titanomagnetite into magnetite-rich and ilmenite or ulvöspinel-rich end-members can occur without significant changes in susceptibility. If such exsolution did not proceed at various times like in the Liverpool flow, but within a few days of moderate backing by the overlying flow, coherent normal polarity direction similar to the above flow could be permanently imprinted in the backed part of the flow, a scenario with similar outcome to what is observed for the top samples of LST and TRC flows.

Finally, we cannot exclude that domain rearrangement within PSD grains played also a role. In a study on recent lava flows from Mt Etna, Calvo *et al.* (2002) heated samples with partly exsolved and unexsolved titanomagnetite and reported on a significant remanence with unblocking temperatures higher than the blocking temperatures. They proposed that high-temperature resistant transdomain remanence resulted from domain rearrangement. Changes in domain state are however difficult to detect as a.f. demagnetization or IRM acquisition tend to affect the magnetic domain state.

de Groot *et al.* (2012) used a multiple specimen protocol to obtain low-field anhysteretic remanent magnetization (ARM) acquisition curves before and after heating steps, without prior (a.f.) removal of the NRM. They showed that, for some Mt. Etna samples, alteration of primary remanence had a magnetic origin resulting from domain rearrangements. Such protocol could not be performed here due to lack of samples. In the current situation, our preferred scenario is that the large remagnetization that was acquired during heating experiments was caused by non-ideal behaviour involving small-scale exsolution and possibly subtle magnetic domain rearrangements.

Whatever the situation and processes involved, remagnetization problems in lava flows are often associated with the presence of unexsolved titanium bearing magnetite. The negative consequence of titanium content on determinations and experiments of absolute palaeointensity has been mentioned and documented for very recent flows (Valet *et al.* 2010). Should we perform palaeointensity experiments from these samples, they would be affected by negative pTRM checks resulting from mineralogical changes during heating. The lower part of the flow appears to be the unique spot that yielded unambiguous magnetic directions carried by pure magnetite grains, and therefore that could be appropriate for determinations of palaeointensity.

9 CONCLUSIONS

Lava flows preceding the last reversal in two sections from the La Palma Island (Spain) have been remagnetized through a large spectrum of unblocking temperatures yielding apparent erroneous transitional directions. We associate this behaviour to the presence of Ti-magnetite with only partial exsolution. Moderate reheating by the overlying flow have reactivated the exsolution of titanomagnetite and raised the Curie temperature of magnetic grains and possibly changed the magnetic domain state of some grains. These effects generated partial remagnetization within about 80 per cent of the flow. This situation differs from other remagnetization features (Coe *et al.* 2014). In the present case, the spurious nature of the palaeomagnetic directions in the interior of the flow was easily detected because lava was emitted before a geomagnetic polarity transition. Such remagnetized components are evidently much more difficult to discern during periods of stable polarity. How frequent is this behaviour remains an open question? It could not be without major impact for studies of palaeosecular variation, absolute palaeointensity and records of short geomagnetic events.

ACKNOWLEDGEMENTS

We thank Andrew Biggin and Yongjae Yu for very insightful comments that greatly improved our manuscript. We are pleased to acknowledge Prof Valera Shcherbakov for fruitful discussions. The research leading to these results has received funding from the European Research Council under the European Union's Seventh Framework Programme (FP7/2007-2013)/ERC advanced grant agreement GA 339899. This is IGP contribution #3848.

REFERENCES

Abdel-Monem, A., Watkins, N.D. & Gast, P.W., 1972. Potassium-argon ages, volcanic stratigraphy, and geomagnetic polarity history of the Canary Islands; Tenerife, La Palma and Hierro, *Am. J. Sci.*, **272**(9), 805–825
 Biggin, A.J., Perrin, M. & Dekkers, M.J., 2007. A reliable absolute palaeointensity determination obtained from a non-ideal recorder, *Earth planet. Sci. Lett.*, **257**(3), 545–563.

Böhnel, H., Morales, J., Caballero, C., Alva, L., McIntosh, G., Gonzalez, S. & Sherwood, G., 1997. Variation of rock magnetic parameters and paleointensities over a single Holocene lava flow, *J. Geomag. Geoelectr.*, **49**(4), 523–542.
 Calvo, M., Prévot, M., Perrin, M. & Riisager, J., 2002. Investigating the reasons for the failure of palaeointensity experiments: a study on historical lava flows from Mt. Etna (Italy), *Geophys. J. Int.*, **149**(1), 44–63.
 Camps, P., Prévot, M. & Coe, R.S., 1995. Revisiting the initial sites of geomagnetic field impulses during the Steens Mountain polarity reversal, *Geophys. J. Int.*, **123**(2), 484–506.
 Coe, R.S. & Prévot, M., 1989. Evidence suggesting extremely rapid field variation during a geomagnetic reversal, *Earth planet. Sci. Lett.*, **92**(3), 292–298.
 Coe, R.S., Prévot, M. & Camps, P., 1995. New evidence for extraordinarily rapid change of the geomagnetic field during a reversal, *Nature*, **374**, 687–692.
 Coe, R.S., Jarboe, N.A., Le Goff, M. & Petersen, N., 2014. Demise of the rapid-field-change hypothesis at Steens Mountain: the crucial role of continuous thermal demagnetization, *Earth planet. Sci. Lett.*, **400**, 302–312.
 Cogné, J.P., 2003. PaleoMac: a Macintosh™ application for treating paleomagnetic data and making plate reconstructions, *Geochem. Geophys. Geosyst.*, **4**(1), doi:10.1029/2001GC000227.
 Day, R., Fuller, M. & Schmidt, V.A., 1977. Hysteresis properties of titanomagnetites: grain-size and compositional dependence, *Phys. Earth planet. Inter.*, **13**(4), 260–267.
 De Boer, C.B. & Dekkers, M.J., 1998. Thermomagnetic behaviour of haematite and goethite as a function of grain size in various non-saturating magnetic fields, *Geophys. J. Int.*, **133**(3), 541–552.
 de Groot, L.V., Dekkers, M.J. & Mullender, T.A., 2012. Exploring the potential of acquisition curves of the anhysteretic remanent magnetization as a tool to detect subtle magnetic alteration induced by heating, *Phys. Earth planet. Inter.*, **194**, 71–84.
 de Groot, L.V., Dekkers, M.J., Visscher, M. & ter Maat, G.W., 2014. Magnetic properties and paleointensities as function of depth in a Hawaiian lava flow, *Geochem. Geophys. Geosyst.*, **15**(4), 1096–1112.
 Dunlop, D.J., 2002. Theory and application of the Day plot (M_{TS}/M_S versus H_{cr}/H_c) 1. Theoretical curves and tests using titanomagnetite data, *J. geophys. Res.*, **107**(B3), doi:10.1029/2001JB000486.
 Dunlop, D.J. & Özdemir, Ö., 2000. Effect of grain size and domain state on thermal demagnetization tails, *Geophys. Res. Lett.*, **27**(9), 1311–1314.
 Fournier, A., Gallet, Y., Usoskin, I., Livermore, P.W. & Kovaltsov, G.A., 2015. The impact of geomagnetic spikes on the production rates of cosmogenic ^{14}C and ^{10}Be in the Earth's atmosphere, *Geophys. Res. Lett.*, **42**(8), 2759–2766.
 Gerya, T., 2009. *Introduction to Numerical Geodynamic Modelling*, Cambridge Univ. Press.
 Hoffman, K.A., 1984. Late acquisition of “primary” remanence in some fresh basalts: a cause of spurious paleomagnetic results, *Geophys. Res. Lett.*, **11**(8), 681–684.
 Jarboe, N.A., Coe, R.S. & Glen, J.M., 2011. Evidence from lava flows for complex polarity transitions: the new composite Steens Mountain reversal record, *Geophys. J. Int.*, **186**(2), 580–602.
 Krása, D., Shcherbakov, V.P., Kunzmann, T. & Petersen, N., 2005. Self-reversal of remanent magnetization in basalts due to partially oxidized titanomagnetites, *Geophys. J. Int.*, **162**(1), 115–136.
 Kruiver, P.P., Dekkers, M.J. & Heslop, D., 2001. Quantification of magnetic coercivity components by the analysis of acquisition curves of isothermal remanent magnetization, *Earth planet. Sci. Lett.*, **189**(3), 269–276.
 Le Goff, M. & Gallet, Y., 2004. A new three-axis vibrating sample magnetometer for continuous high-temperature magnetization measurements: applications to paleo- and archeo-intensity determinations, *Earth planet. Sci. Lett.*, **229**(1), 31–43.
 Mankinen, E.A., Prévot, M., Grommé, C.S. & Coe, R.S., 1985. The Steens Mountain (Oregon) geomagnetic polarity transition 1. Directional history, duration of episodes, and rock magnetism, *J. geophys. Res.*, **90**(B12), 10 393–10 416.

- Middleton, M. & Schmidt, P.W., 1982. Paleothermometry of the Sydney basin, *J. geophys. Res.*, **87**(B7), 5351–5359.
- Moon, T. & Merrill, R.T., 1986. A new mechanism for stable viscous remanent magnetization and overprinting during long magnetic polarity intervals, *Geophys. Res. Lett.*, **13**(8), 737–740.
- Néel, L., 1955. Some theoretical aspects of rock-magnetism, *Phil. Mag. Suppl.*, **4**, 191–243.
- O'Reilly, W., 1984. *Rock and Mineral Magnetism*, Blackie, Chapman & Hall, p. 220.
- Prévot, M., Mankinen, E.A., Coe, R.S. & Grommé, C.S., 1985. The steens mountain (Oregon) geomagnetic polarity transition: 2. Field intensity variations and discussion of reversal models, *J. geophys. Res.*, **90**(B12), 10 417–10 448.
- Pullaiah, G., Irving, E., Buchan, K.L. & Dunlop, D.J., 1975. Magnetization changes caused by burial and uplift, *Earth planet. Sci. Lett.*, **28**(2), 133–143.
- Quidelleur, X. & Valet, J.P., 1996. Geomagnetic changes across the last reversal recorded in lava flows from La Palma, Canary Islands, *J. geophys. Res.*, **101**(B6), 13 755–13 773.
- Sagnotti, L., Scardia, G., Giaccio, B., Liddicoat, J.C., Nomade, S., Renne, P.R. & Sprain, C.J., 2014. Extremely rapid directional change during Matuyama-Brunhes geomagnetic polarity reversal, *Geophys. J. Int.*, **199**(2), 1110–1124.
- Shaw, H.R., Hamilton, M.S. & Peck, D.L., 1977. Numerical analysis of lava lake cooling models; Part I, Description of the method, *Am. J. Sci.*, **277**(4), 384–414.
- Thellier, E. & Thellier, O., 1944. Recherches géomagnétiques sur des coulées volcaniques d'Auvergne, *Ann. Geophys.*, **1**, 37–52.
- Valet, J.P., Kidane, T., Soler, V., Brassart, J., Courtillot, V. & Meynadier, L., 1998. Remagnetization in lava flows recording pretransitional directions, *J. geophys. Res.*, **103**(B5), 9755–9775.
- Valet, J.P., Herrero-Bervera, E. & Carlut, J., 2010. A selective procedure for absolute paleointensity in lava flows, *Geophys. Res. Lett.*, **37**, L16308, doi:10.1029/2010GL044100.
- Watkins, N.D., 1965. Paleomagnetism of the Columbia plateaus, *J. geophys. Res.*, **70**(6), 1379–1406.
- Zijderveld, J.D.A., 1967. AC demagnetization of rocks: analysis of results, in *Methods in Palaeomagnetism*, pp. 254–286, Collinson, D.W., Creer, K.M. & Runcorn, S.K., Elsevier, New York.

SUPPORTING INFORMATION

Supplementary data are available at [GJI](#) online.

Figure S1. Alternating field and thermal demagnetization diagrams of twin specimens. The characteristic components isolated by both methods are almost identical.

Figure S2. Day plots (Day *et al.* 1977) of samples located from bottom to top within flows LST and TRC. Overall there is no marked evolution within flows. MD/SD mixing curves are from Dunlop (2002).

Figure S3. Viscosity index of samples from flows LST and TRC. The index was calculated after storing the samples for two weeks. Largest values are found in the middle of the flow.

Please note: Oxford University Press is not responsible for the content or functionality of any supporting materials supplied by the authors. Any queries (other than missing material) should be directed to the corresponding author for the paper.